© 2021. Published by The Company of Biologists Ltd | Journal of Experimental Biology (2021) 224, jeb239178. doi:10.1242/jeb.239178

RESEARCH ARTICLE

Departures from isotropy: the kinematics of a larval snail in response to food

Michelle H. DiBenedetto[1,2,3,*], Kirstin S. Meyer-Kaiser[1], Brooke Torjman[4], Jeanette D. Wheeler[1,5] and Lauren S. Mullineaux[1]

ABSTRACT

The swimming behavior of invertebrate larvae can affect their dispersal, survival and settlement in the ocean. Modeling this behavior accurately poses unique challenges as behavior is controlled by both physiology and environmental cues. Some larvae use cilia to both swim and create feeding currents, resulting in potential trade-offs between the two functions. Food availability is naturally patchy and often occurs in shallow horizontal layers in the ocean. Also, larval swimming motions generally differ in the horizontal and vertical directions. In order to investigate behavioral response to food by ciliated larvae, we measured their behavioral anisotropy by quantifying deviations from a model based on isotropic diffusion. We hypothesized that larvae would increase horizontal swimming and decrease vertical swimming after encountering food, which could lead to aggregation at food layers. We considered *Crepidula fornicata* larvae, which are specifically of interest as they exhibit unsteady and variable swimming behaviors that are difficult to categorize. We tracked the larvae in still water with and without food, with a portion of the larvae starved beforehand. On average, larvae in the presence of food were observed higher in the water column, with higher swimming speeds and higher horizontal swimming velocities when compared with larvae without food. Starved larvae also exhibited higher vertical velocities in food, suggesting no aggregation behavior. Although most treatments showed strong anisotropy in larval behavior, we found that starved larvae without food exhibited approximately isotropic kinematics, indicating that behavioral anisotropy can vary with environmental history and conditions to enhance foraging success or mitigate food-poor environments.

KEY WORDS: Zooplankton swimming, Invertebrate larvae, Foraging

INTRODUCTION

Many benthic marine invertebrates reproduce through a planktonic larval phase. The dispersal and ultimate settlement of the larvae are influenced by both environmental and behavioral factors (Cowen and Sponaugle, 2009; Pineda and Reyns, 2018). Individual larvae can exhibit a wide variety of behaviors that are controlled by both their morphology and environmental cues (Young and Vazquez, 1995; Chan, 2012). The behavior of larvae at the scale of the individual can affect their ability to find and identify a suitable habitat, settle and survive (Young and Chia, 1984; Koehl, 2007), whereas at the scale of the population, larval behavior affects dispersal patterns (Metaxas, 2001). Larval behavior is not expected to be isotropic, as environmental and ecological motivations differ in each direction in the ocean. For example, upward and downward motion are associated with settlement, and horizontal motion is associated with dispersal. However, the influences of foraging and feeding on the anisotropy of larval behavior are not obvious.

Many invertebrate larvae are ciliated, beating their cilia both to swim and to feed, resulting in potential interactions and trade-offs between these two actions (Emlet et al., 1985). Larvae have been described as 'good eaters, but poor swimmers' owing to compromises in larval form, as increases with feeding efficiency are often met with decreases in propulsion and swimming efficiency (Strathmann and Grünbaum, 2006). Observations of the flow induced by bat star larvae indicate that some ciliated larvae may switch between feeding and swimming modes to address this trade-off, resulting in slower swimming while feeding (Gilpin et al., 2017). This suggests that the free-swimming behavior of larvae may be influenced by food availability, and that larvae may swim slower while feeding. However, these observations were of confined larvae, and therefore open questions remain regarding how their results translate to free-swimming larvae (von Dassow et al., 2017).

Molluscan veliger larvae have been the subject of many studies of larval behavior; they have opposed bands of cilia which they use to swim and feed (Pernet, 2018). Observations of veligers show they can mediate their food intake and reject food particles (Gallager, 1988). Although the exact mechanisms by which they decouple feeding and swimming remain elusive, their ability to separate the two functions suggests the larvae may be able to potentially minimize any trade-offs (Strathmann et al., 2019). In this study, we specifically consider the veliger larvae of the gastropod *Crepidula fornicata* as a model system. Although ciliary beating can control the strength of swimming and feeding currents, *C. fornicata* are of interest because their swimming speed does not directly correlate with their ciliary beating (Chan et al., 2013), but rather with velum extension and position. This suggests that swimming–feeding trade-offs in ciliated veligers may provide new insights when compared with other organisms.

Another defining characteristic of veliger behavior is that it is inherently anisotropic, as gravity passively induces a stable preferential orientation. Their heavy shells induce an 'upright' posture with their shell oriented downwards, and their velum oriented upwards (Kessler, 1986; Fuchs et al., 2015); veligers produce propulsion in the direction of their velum, thus they are biased toward upward swimming. In addition, they are negatively buoyant and must therefore exert a minimum swimming propulsion to keep from settling downward. In this way, downward transport

[1]Biology Department, Woods Hole Oceanographic Institution, Woods Hole, MA 02543, USA. [2]Physical Oceanography Department, Woods Hole Oceanographic Institution, Woods Hole, MA 02543, USA. [3]Mechanical Engineering Department, University of Washington, Seattle, WA 98115, USA. [4]Muhlenberg College, Allentown, PA 18104, USA. [5]Institute of Environmental Engineering, Department of Civil, Environmental, and Geomatic Engineering, ETH Zürich, 8093 Zürich, Switzerland.

*Author for correspondence (mdibenedetto@whoi.edu)

M.H.D., 0000-0003-2657-1971

Received 15 October 2020; Accepted 13 November 2020

Journal of Experimental Biology (2021) 224, jeb239178. doi:10.1242/jeb.239178

can be due to passive sinking, whereas maintaining a constant vertical position necessitates active swimming. Horizontal movement relative to the fluid environment must be due to active swimming. Therefore, if a larva is swimming upward at a constant rate, and it reorients horizontally, the vertical component of the larva's motion will decrease or reverse and the larva will sink unless it increases its overall swimming speed. This suggests that any increase in relative horizontal motion may be met with changes in vertical motion.

Larval behavior is also affected by the anisotropy of the ocean environment. Light and nutrient availability are often stratified, with food being patchy and potentially distributed in thin horizontal layers. Ocean currents are depth-dependent as well. Therefore, larvae exhibit inherently anisotropic behavior, a topic that has been of general interest to zooplankton behavioral ecology (e.g. Yen 1988; Mahjoub et al. 2011; Schuech and Menden-Deuer 2014). In terms of transport, vertical swimming alters a larva's position in the water column, which can control horizontal transport in sheared oceanic or tidal currents (Shanks, 1995; McManus and Woodson, 2012). Vertical swimming occurs during ontogenetic or daily vertical migrations. Downward swimming reduces dispersal of larvae, as they are exposed to slower flow in the benthic boundary layer (Shanks, 2009). Horizontal swimming of small larvae is not necessarily strong enough to affect net transport when compared with oceanic currents (Porch, 1998), but at slow flow speeds in lagoons or near benthic substrata, horizontal swimming can affect settlement location (e.g. Butman et al., 1988; Bingham and Young, 1991; Maciejewski et al., 2019). Horizontal swimming is associated with feeding in thin layers (Menden-Deuer and Grünbaum, 2006) and food patches (Metaxas and Young, 1998; Sameoto and Metaxas, 2008). Other behaviors, such as diving or swimming in helices, may be used for feeding, predator avoidance or in response to physical or chemical cues (Fuchs et al., 2004; Fuchs et al., 2018; Wheeler et al., 2015, 2017; Maciejewski et al., 2019).

Owing to anisotropic environmental influences in the ocean, morphological constraints, and the intrinsic link between swimming and feeding in ciliated larvae, larval behavior is expected to exhibit varying levels of anisotropy. We propose measuring this anisotropy under controlled cues to investigate the response of veliger larvae to food. In this study, we specifically evaluated the behavior of larvae of the common slipper limpet, *C. fornicata*. This species has been studied as a model system for developmental and larval biology (Henry et al., 2010) and has previously been observed to exhibit highly variable swimming speeds and behaviors (Chan et al., 2013). We exposed fed and starved *C. fornicata* larvae to still-water flasks with and without food, in order to quantify and describe differences in larval behavior that may be related to feeding–swimming trade-offs. We analyzed the distributions of their kinematics, and employed behavioral anisotropy as an indicator to characterize behavioral response. We expected that the anisotropy of their behavior would change in the presence of food, with larvae exhibiting more horizontal motion while feeding. An increase in horizontal motion is expected to occur with a decrease in vertical motion. Any change to vertical motion is expected to change the vertical distributions of larvae as well. Finally, we expected that any food-mediated response in behavior would be more prevalent in starved larvae.

MATERIALS AND METHODS

Culturing

Adult *Crepidula fornicata* (Linnaeus 1758) were collected in Vineyard Sound, MA, USA. Stacks of individuals were collected from 30 m depth and were transported to Woods Hole Oceanographic Institution. Adults spawned on 2 July 2018 after spending approximately 1 week in captivity, and larvae were collected within 24 h by reverse filtration with 150 µm mesh.

Larval *C. fornicata* were cultured in clean 2 liter glass jars, which were filled to 1.5 liters with 0.2- µm filtered seawater. Every day, larvae were transferred to clean jars and fed with a Tahitian strain of *Isochrysis galbana*, resulting in a concentration of 1.8×10^5 cells ml^{-1}. This concentration was also maintained as the food source in the swimming experiments. After a week in culture, larvae were split into fed and starved treatments, with fed larvae continuing to be fed as normal and starved larvae receiving no food for 4 days prior to the experiment. The experiments were conducted 9 days post hatch. The diameters of the larvae were measured under a dissecting microscope. The fed and starved larvae measured on average 522±9 and 508±6 µm, respectively.

Experimental setup

To isolate the larval response to the presence of food, we conducted experiments that manipulated only food availability and history of starvation. Many other external variables can affect larval behavior, such as light, temperature, salinity, predators and flow cues. We have excluded those variables in our experiment, yet cue hierarchies undoubtedly exist and should be investigated further.

Behavioral experiments were conducted for fed (Fed) and previously starved (St) larvae, either in the presence of food (F) or without food (0) in filtered seawater, resulting in four distinct treatments. The food levels in the F treatments were at a satiating concentration level, identical to the level used in culturing the larvae. For each treatment, five replicate experiments were conducted. Each replicate contained observations of approximately nine to 16 individual larvae, resulting in concentrations of 0.18–0.32 larvae ml^{-1}. For each treatment, the total number of larvae observed across all five replicates was 72, 66, 70 and 62 individuals in the St-0, St-F, Fed-0 and Fed-F treatments, respectively. The experiments were run over long enough times that the larvae could swim the length of the flask multiple times in the observation period, resulting in converged kinematic distributions. The sequence of replicate flasks and environmental treatments was randomized using a random number generator.

All larval swimming observations were conducted in a temperature-controlled chamber at 20°C in the dark to eliminate any thermal or phototactic influences on larval behavior. Each experimental trial was conducted in a new 65 ml flat-sided flask; the flasks measured 4.5 cm wide, 2.3 cm deep and 6.1 cm tall. The flask was filled to a depth of 5 cm with filtered seawater (no food) or well-mixed *I. galbana* in filtered seawater (food). *Crepidula fornicata* larvae were concentrated into a small volume of water and introduced to the experimental flasks on a small piece of 100 µm mesh, which was inserted into the flask with forceps. The flask was illuminated from behind with a diffuse near-infrared LED array (Olymstore, 12 V, 2A, 850 nm), and larval swimming behaviors were recorded over 5 min at 30 frames s^{-1} with a CMOS camera (Basler acA2040-90umNIR). The recorded field of view focused on the center plane of the flask, and showed a vertical cross-section of the flask that included the full vertical and horizontal extent of the flask.

Larval tracking

Video observations of larval behavior were recorded as a series of .tiff images, which were used for particle tracking. Larval centroids were identified in the images with MATLAB, and the *x*- and

Journal of Experimental Biology (2021) 224, jeb239178. doi:10.1242/jeb.239178

z-positions and horizontal and vertical (u,w) velocities of each larva in each frame were evaluated with particle-tracking algorithms based on Kelley and Ouellette (2011), which use a predictive algorithm to link trajectories and a Gaussian smoothing and differentiation kernel to calculate velocities. The angular velocity ω of each larva in each frame was calculated based on the rate of change of the swimming direction. Example trajectories and raw video footage for each treatment are shown in Fig. S1 and Movies 1 and 2.

The particle-tracking velocities calculated for each larva represent the resultant velocities of the larvae, based on the combined propulsive swimming force, gravitational force and hydrodynamic forces such as drag and added mass. Therefore, the direction of the larval motion is not necessarily the direction of their swimming propulsion alone (see Fuchs et al., 2013). Swimming indicates an active response, whereas larvae sink passively; therefore, observed larval speed is not necessarily proportional to larval swimming strength. Because of the small Reynolds number of *C. fornicata* larvae and the still water in which they were observed, we assume the hydrodynamic forces are much smaller than the forces owing to gravity and propulsion. Therefore, we assume all horizontal behavior is due solely to active swimming, and vertical behavior is due to swimming plus a constant gravitational force that is a function of the larval size and density.

From the larval velocity measurements, we also assessed the direction of larval motion. Direction was calculated as the arctangent of the instantaneous velocity ratio w/u. The directional behavior of the larvae was assessed by the comparison of the probability density functions (PDFs) of their movement direction for each treatment. To isolate strictly horizontal and vertical behaviors, we calculated the fractions F_{horiz} and F_{vert} of direction observations within 15 deg of (0 deg, 180 deg) and (90 deg, 270 deg), respectively. Confidence intervals were quantified by bootstrapping the data (Efron, 1979).

After the larvae were introduced to the flask, there was an adjustment period of approximately 10 s, during which most individuals went to the bottom of the flask. This time period was excluded from our analysis. In many instances, larvae that encountered the upper free surface of the water repeatedly dipped below it and re-approached it (as seen in Fig. S1D). Larvae at the free surface and on the bottom of the flask were also difficult to track owing to imaging interference based on refraction of light by the clear flask. Therefore, trajectory segments that were within 1 cm of the top or bottom of the flask were excluded from the kinematic analyses.

Many studies of larval behavior focus on either distinct behaviors (diving, helices) or point-statistics such as average swimming speed (Meyer et al., 2018; Maciejewski et al., 2019). However, these statistics lack complexity, which can be important for accurately reproducing the observed distributions of larvae (e.g. Daigle and Metaxas, 2012). Many larval behaviors fall along a continuum, so instead of classifying individual trajectories, we used aggregate statistical approaches to classify behavioral differences. We treated each instantaneous value of horizontal velocity, vertical velocity, angular velocity and speed as a single data point and constructed PDFs of these parameters. This resulted in over 10,000 data points for each treatment, pooled across all replicates.

Vertical distribution of larvae

The vertical distribution of larvae was assessed by calculating the vertical centroid $\langle z \rangle$ of the observed trajectories. For each of the five replicates for each treatment, the average vertical position was calculated for all tracks over the last minute of the observational period, resulting in five data points per treatment. All larval trajectory data were used; larvae that disappeared from the field of view, either by approaching the top of the flask or the bottom, were assumed to stay at their respective vertical location until they reappeared. Note that no velocity data were available for the larvae after they had disappeared from the field of view. The validity of this approach was confirmed by visually inspecting the raw images. To test for significant differences in larval position in the water column, we used a two-way crossed ANOVA with fed/starved and with/without food as factors, plus the interaction. A Tukey test was used for pairwise *post hoc* tests.

Statistical analysis of larval kinematics

Velocity data for larvae in each treatment were analyzed in aggregate. Individuals had a range of velocities, which were characterized by calculating PDFs for velocity values in each treatment. For each velocity distribution, we calculated the root mean square (RMS) to characterize the overall magnitude and spread of velocity behavior. We do not report mean directional velocity values, as the horizontal velocity mean values were approximately zero, and the vertical behavior of the larvae was constrained by the flask. The RMS statistics were bounded by 95% confidence intervals (CI), which were calculated by bootstrapping the data (Efron, 1979).

We compared the velocity data with an ideal model of isotropic behavior in order to quantify the degree of anisotropy. The model is based in a model of diffusion (Okubo, 1994); however, owing to the confined nature of the experiments, total diffusion (dispersal) of the larvae could not be directly quantified, as the larvae eventually encountered the boundaries of the flask. A diffusion model assumes the larvae disperse based on a diffusion coefficient $D \approx U^2\tau$, where U is a characteristic velocity scale and τ is the correlation time scale of the larval motion, which can be thought of as a turning timescale (Porch, 1998; Visser and Kiørboe, 2006). Instead of approximating D, we report velocity kinematics directly. We assumed that isotropic diffusion of the larvae would result in normally distributed velocity distributions, leading to larvae that diffuse in all directions uniformly. From normally distributed velocities, it follows that the distribution of larval absolute speed would follow a Maxwell–Boltzmann distribution, which we employed to characterize total larval speed.

In order to assess the degree of normalcy in the velocity distributions, we standardized larval velocities by subtracting the mean and normalizing by the standard deviation σ, e.g. standardized horizontal velocity is denoted as $\hat{u}$, where $\hat{u} = (u - \langle u \rangle)/\sigma_u$, where $\langle u \rangle$ symbolizes average horizontal velocity, with standardized vertical velocity $\hat{w}$ calculated in a similar manner. The quantities $\hat{u}$ and $\hat{w}$ were calculated to compare the observed distributions to the expectations of the Gaussian distributions, in which the PDF of one velocity component $p(u)$ is normally distributed, such that:

$$p(u) = \frac{1}{\sigma\sqrt{2\pi}} \exp(-u^2/2\sigma^2), \quad (1)$$

with standard deviation σ and a mean of zero. In the case of a distribution with zero mean, $\sigma_u \approx u_{\text{RMS}}$. We measured only two components of velocity in our experiments, horizontal u and vertical w. Thus, the speeds calculated are a two-dimensional projection of the full three-dimensional speed. In two dimensions, the PDF of the speed $V = \sqrt{u^2 + w^2}$ is given by a two-dimensional

Journal of Experimental Biology (2021) 224, jeb239178. doi:10.1242/jeb.239178

Maxwell–Boltzmann distribution:

$$p(V) = \frac{V}{\sigma^2}\exp(-V^2/2\sigma^2). \quad (2)$$

It follows that the expected value of V is $\sqrt{2/\pi}\sigma$, and thus only σ is needed to characterize the magnitude of the distribution. To compare speeds between treatments, the observed V PDFs were fit to Eqn 2 with σ as the fitting parameter. The curve-fitting was conducted by minimizing the mean squared error weighted by Eqn 2. This process was repeated recursively until the value of σ converged for each treatment.

Differences between observed PDFs f and expected PDFs f_0 were assessed with the χ^2 statistic, defined as:

$$\chi^2 = \sum_i \frac{(f(i) - f_0(i))^2}{f_0(i)}, \quad (3)$$

where $\Sigma_i f(i) = \Sigma_i f_0(i) = 1$. Note that this formulation of χ^2 is independent of sample size, and thus allows for direct comparison between distributions with variable sample sizes. For each distribution, we used the same binning to calculate Eqn 3. Uncertainty of χ^2 is assessed by bootstrapping the data to yield 95% CI. For identical distributions, $f = f_0$ and $\chi^2 = 0$; the larger the value of χ^2, the larger the difference between the distributions.

RESULTS

Kinematics

The observed velocity (u,w) PDFs for each treatment are plotted in Fig. 1. The horizontal velocity u distributions (Fig. 1A) follow symmetric, normal distributions much more closely than those of the vertical velocity w (Fig. 1B), where the latter display more off-center peaks and asymmetry. We quantitatively assessed the degree of normalcy in the distributions with the χ^2 statistic, reported in Table 1. Across all treatments, χ^2 of u is lower than for w, which indicates that larval swimming velocities in the vertical direction deviate more strongly from a normal distribution than in the horizontal. The lowest χ^2 values for $\hat{u}$ and $\hat{w}$ occur for the St-0 treatment, indicating that the St-0 treatment exhibited larvae with velocity behavior that best agrees with a normal distribution.

In comparing the velocity distributions across treatments, the horizontal velocity distributions follow a clear pattern, whereas the distributions of the vertical velocity are more complicated. There is a higher degree of spread, and a larger range of velocities for the horizontal velocity u of the Fed treatment larvae when compared with the starved (St) treatment, as well as with the presence of food (F) in both treatments. With respect to the vertical velocity w distributions, the Fed treatments also show more spread and a larger range of velocities when compared with the St treatments. Also, the St-F treatment exhibits a larger range of both upward (positive) and downward (negative) vertical velocities when compared with the St-0 treatment. Similar faster vertical velocities are observed for the Fed-F treatment compared with the Fed-0 treatment, but only for the downward velocities. The upward vertical velocities show similar ranges of values for both Fed treatments, with a peak of fast upward velocities in the Fed-F treatment. Owing to the large sample sizes of each data set, all calculated distributions are significantly different from each other and the normal distribution with P-values <0.001 (Pearson's chi-squared test).

Table 1. Characterization of how normally distributed the velocity distributions are for each treatment: starved larvae without and with food (St-0, St-F), and fed larvae without and with food (Fed-0, Fed-F)

	χ^2	
	$\hat{u}$	$\hat{w}$
St-0	0.011	0.051
St-F	0.020	0.23
Fed-0	0.025	0.17
Fed-F	0.036	0.071

χ^2 statistics for the standardized velocity ($\hat{u}$, $\hat{w}$) are calculated with respect to the standard normal curve (Eqn 1).

Absolute observed two-dimensional speed V PDFs for each treatment are shown in Fig. 2A. To further characterize and compare the curves, best fits to the data for the two-dimensional Maxwell–Boltzmann distribution are shown in Fig. 2B, with the fitting parameters reported in Table 2. The fitted distribution parameter σ characterizes the overall speed of the larvae for each treatment. Comparing σ between treatments allows us to quantify the response of the larvae to the presence of food in both feeding history cases. In response to food, an increase in total larval speed is seen with similar magnitude for both starved and fed larvae, $\Delta\sigma = 0.0078$ and 0.0068 cm s^{-1}, respectively, suggesting that the increase in larval speed owing to the presence of food is not dependent on whether the larvae were previously starved. The data also show that the starved larvae on average move at slower speeds than the fed larvae.

The horizontal and vertical larval velocities are further assessed by calculation of the RMS values, plotted in Fig. 3A. The St-0 larvae have the lowest u_{RMS} and w_{RMS} values out of all treatments, which agrees with the observation that they had the lowest absolute speeds. The St-F larvae have higher u_{RMS} and w_{RMS} relative to the St-0 treatment, so the presence of food increases larval speed in both the horizontal and vertical directions for the starved larvae. The increase in horizontal speeds must be a direct result of increased horizontal swimming, but the increased vertical speed could be due to both higher vertical swimming speeds, as well as faster passive sinking. The fed larvae show similar trends in the horizontal velocities: u_{RMS} for the Fed-F treatment is larger than u_{RMS} of the Fed-0 treatment. However, there is no difference between w_{RMS} owing to the presence of food for the fed larvae. Therefore, we see that the presence of food increases the magnitude of observed

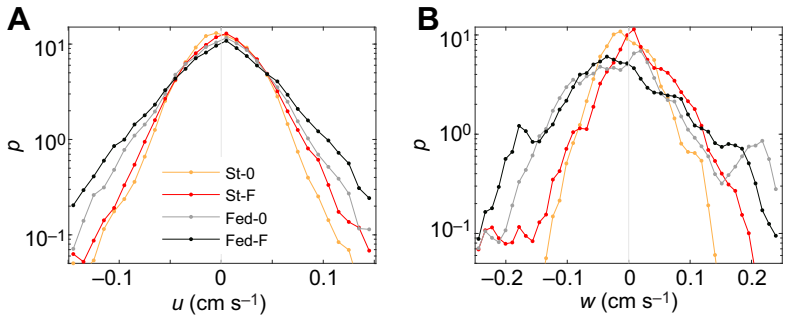

Fig. 1. Horizontal (u) and vertical (w) velocity probability density functions (PDFs) for each treatment. Probability density is denoted as p. Light data points (orange, grey) correspond to treatments without food (0), and dark data points (red, black) correspond to treatments with food (F). Previously starved (St) larvae are in orange and red, whereas fed (Fed) larvae are in grey and black. The vertical light grey line in each plot indicates zero velocity.

Journal of Experimental Biology (2021) 224, jeb239178. doi:10.1242/jeb.239178

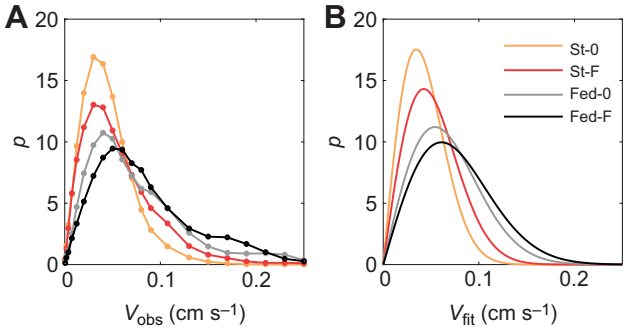

Fig. 2. Larval speed PDFs across treatments. PDFs (A) of the data (V_{obs}) and (B) from best fits to the data (V_{fit}) with Eqn 2. The fitting parameter σ for each curve in B is shown in Table 2. Treatments shown include previously starved larvae without or with food (St-0, St-F), and previously fed larvae without or with food (Fed-0, Fed-F).

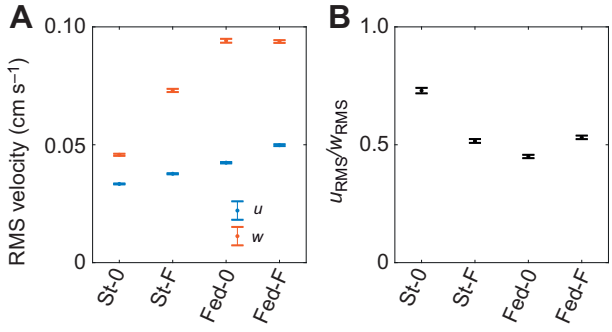

Fig. 3. Larval velocity statistics across treatments. (A) Measured root mean square (RMS) horizontal (*u*) and vertical (*w*) velocities for each treatment, and (B) the ratio of the two. Error bars show 95% confidence intervals. The four treatments correspond to starved larvae without or with food (St-0, St-F), and previously fed larvae without or with food (Fed-0, Fed-F).

horizontal velocity for both fed and starved larvae, but only increases the observed vertical velocity for the starved larvae.

In order to assess anisotropy of larval motion, we compared horizontal and vertical RMS velocities for each treatment. The ratio u_{RMS}/w_{RMS} is shown in Fig. 3B. A ratio close to 1 indicates isotropic behavior. By this definition, the St-0 treatment has the most isotropic larval behavior, while larvae in the St-F, Fed-0 and Fed-F treatments have more anisotropic behaviors, with the ratio $u_{RMS}/w_{RMS}\approx0.5$ for the St-F, Fed-0 and Fed-F larvae treatments. Therefore, the larvae are moving approximately twice as fast in the vertical as in the horizontal direction. In all cases, the ratio $u_{RMS}/w_{RMS}<1$, indicating that all of the larvae observed on average move faster vertically than horizontally.

Vertical distribution of larvae

Another measure of larval behavior is their vertical distribution in the water column. This is assessed by comparing the mean vertical position of larvae $\langle z\rangle$, which varies by treatment, as shown in Fig. 4. Higher $\langle z\rangle$ values indicate that larvae are higher in the water column. Starved larvae without food remained near the bottom of the flask, but larvae were significantly higher in the water column when fed (ANOVA, d.f.=1, F=5.96, P=0.02) and when in the presence of food (ANOVA, d.f.=1, F=16.3, P<0.001). There was no significant interaction of fed/starved or with/without food (ANOVA, d.f.=1, F=0.49, P=0.49). Pairwise *post hoc* tests revealed significant differences between the treatments St-0 and St-F (P=0.01) and St-F and Fed-0 (P=0.001). These findings show that when food was present, larvae were found higher in the water column, and that this relationship was strongest for the starved larvae.

Directional behavior

The PDFs of larval movement direction are plotted for each treatment in Fig. 5A. In both Fed treatments (Fed-0 and Fed-F), larvae are observed traveling downward the majority of the time. Larvae in the St-0 and St-F treatments have a higher fraction of observed horizontal motion, with the largest horizontal peak in the St-F treatment.

Directional behavior is further quantified in Fig. 5B, where the exact fractions of observations of horizontal and vertical movement (F_{horiz}, F_{vert}) are reported for each treatment. In terms of horizontal movement, while the presence of food does increase F_{horiz} in both the starved and fed larvae, the largest increase is seen in the starved larvae, where the St-F treatment has the highest value of F_{horiz} of all treatments. The fraction of vertical movement is also shown for reference, which is also seen to increase from the St-0 to St-F treatments, with no change seen between the Fed-0 and Fed-F treatments. These observations indicate that, especially for the starved larvae, the presence of food increases the frequency of horizontal motion, but in all treatments, the fraction of horizontal motion remains less than that of vertical motion.

Isotropy of the directional PDFs is assessed by comparing the distributions to a uniform distribution, quantified through χ^2, reported in Table 3. A lower χ^2 value indicates higher isotropy. Therefore, the St-0 treatment has the most isotropic directional behavior, with almost equal probability of larvae swimming in every direction. The χ^2

Table 2. Speed PDF parameter for each treatment, found from the best fits to Eqn 2 shown in Fig. 2

	V_{fit}	
	σ (10^{-2} cm s^{-1})	95% CI
St-0	3.46	[3.43, 3.49]
St-F	4.24	[4.06, 4.40]
Fed-0	5.41	[5.16, 5.65]
Fed-F	6.09	[5.89, 6.28]

The parameter σ and 95% confidence intervals (CI) are reported.

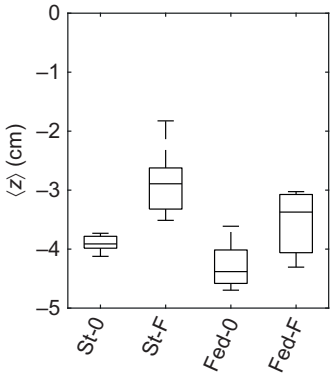

Fig. 4. Box plots of averaged vertical centroid ⟨z⟩ of larvae tracks across treatments, aggregated by replicate. The water surface at the top of the flask corresponds to z=0. Treatments shown include previously starved larvae without or with food (St-0, St-F), and previously fed larvae without or with food (Fed-0, Fed-F). Differences between treatments were found to be statistically significant for St-0 and St-F (P=0.01) and St-F and Fed-0 (P=0.001) with a pairwise *post hoc* ANOVA test. Data for each treatment are the average centroid from each of the five replicate experiments per treatment.

Journal of Experimental Biology (2021) 224, jeb239178. doi:10.1242/jeb.239178

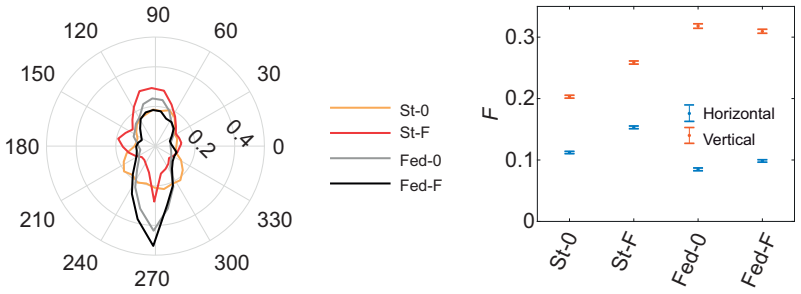

Fig. 5. Directional larval velocity statistics across treatments. (A) Swimming direction PDFs for all treatments, with azimuthal axis denoted in degrees and radial axis in probability density. An angle of 90 deg corresponds to upward motion and 270 deg corresponds to downward motion. (B) Fraction *F* of observations of larvae moving in either the horizontal or vertical direction in each treatment. Error bars show 95% confidence intervals. The treatments shown are for starved larvae without or with food (St-0, St-F), and previously fed larvae without or with food (Fed-0, Fed-F).

values show that the presence of food increases larval directional anisotropy in all treatments. Furthermore, starved larvae have more isotropic behavior when compared with the fed larvae treatments.

Vertical anisotropy

To further assess the larval vertical behavior, we divided the observations in each treatment into upward and downward moving. We compared absolute speed V and angular velocity ω for each case in each treatment (Figs 6 and 7). Larvae in the St-0 treatment had almost identical speed and angular velocity distributions when moving upward and downward (Figs 6A and 7A), indicating a strong isotropy in larval vertical behavior. This symmetry breaks down, however, in the presence of food: the St-F speed distributions differ between upward- and downward-moving larvae (Fig. 6B). This result shows that the presence of food can increase behavioral anisotropy.

For both starved and fed larvae in the presence of food, there is a higher peak in the PDF at lower speeds for downward moving relative to that of upward moving. This peak indicates that larvae are more often moving slowly going down than when going up. In all treatments except St-0, there are strong differences in the shapes of the speed PDFs between upward and downward movement. We also calculated and plotted mean absolute horizontal velocities $\langle|u|\rangle$ and vertical velocities $\langle|w|\rangle$ for the upward- and downward-moving larvae for each treatment in Fig. 6C,F. In all but the St-0 treatment, the upward mean horizontal velocities are higher than the downward velocities, with the difference being the largest in the Fed-F treatment (see Fig. 6C). The differences in the mean absolute vertical velocities are less dramatic, with higher speeds downward in the St-F and Fed-0 treatments, and approximately equal upward and downward speeds in the St-0 and Fed-F treatments (see Fig. 6F). These differences are small, do not show a clear trend, and do not provide as much information as the whole PDFs.

Angular velocity PDFs are nearly identical for upward- and downward-moving larvae in the St-0 and St-F treatments, indicating strong angular isotropy for these larvae. Overall, differences in angular velocity between treatments are small, as shown from total ω_{RMS} in Fig. 7F. However, differences in angular velocity ω are apparent between upward- and downward-moving larvae in the Fed-0 and Fed-F treatments, as shown in Fig. 7D,E; the tails of the distributions for ω are higher for upward-moving larvae than for downward-moving larvae in these treatments. The ω_{RMS} values differ between upward- and downward-moving larvae in the Fed-0 and Fed-F treatments, reinforcing this result (Fig. 7C). These results show that fed larvae turn more as they swim up, which could be related to feeding or exploratory behavior. It is also likely related to the fact that downward motion is more passive than upward motion.

Table 3. Characterization of how uniformly distributed the direction distributions are for each treatment represented by χ^2 statistics for the direction PDFs in Fig. 5A with respect to the uniform distribution

	χ^2	95% CI
St-0	0.065	[0.062, 0.067]
St-F	0.15	[0.14, 0.16]
Fed-0	0.29	[0.28, 0.30]
Fed-F	0.35	[0.34, 0.36]

95% confidence intervals (CI) are also reported.

DISCUSSION

We assessed the swimming behaviors of *C. fornicata* larvae in response to food by measuring the deviations from a model that assumes isotropic kinematics, normally distributed directional velocities, and a uniform directional distribution. The larvae were observed in still-water flasks either with or without food, and were either previously fed or starved. Our results revealed anisotropic larval behavior across treatments, as expected. However, we did observe largely isotropic behaviors in the St-0 treatment (starved larvae without food), indicated by: (i) normally distributed horizontal and vertical velocities, (ii) similar magnitude of horizontal and vertical velocities, (iii) similar distributions of upward and downward speeds, and (iv) the most uniform velocity direction distribution of all treatments. Therefore, we found that an isotropic diffusion model of behavior is a good approximation for the observed starved *C. fornicata* larvae without food. In other words, in the absence of food, previously starved larvae tend to move in all directions with equal probability and similar speed.

However, in the field, larvae are rarely – if ever – completely starved and without food. Our results showed increased behavioral anisotropy for larvae that were fed and in the presence of food. Food sources in the environment are patchy, both horizontally and vertically (Daro, 1988). Because of this environmental variability, larvae may constantly readjust their behaviors based on their immediate surroundings, thus influencing dispersal and settlement. Our findings further indicate that the anisotropy of the larval behavior is not static, and may be another useful parameter in quantifying behavioral response.

The observed increase in both magnitude and frequency of horizontal swimming in response to food may be motivated by the fact that phytoplankton are often present in thin horizontal layers in the environment (Durham and Stocker, 2012). An increase in horizontal swimming, and a corresponding decrease in vertical movement, would increase larval residence times and aggregation at a specified depth. Changes in the kinematics of plankton in response to thin layer cues have been observed in laboratory settings. Aggregation behavior was observed in heterotrophic dinoflagellates in still water, where an increase in both horizontal motion and swimming speed, and a decrease in vertical velocity, were observed in the presence of a thin layer food cue (Menden-Deuer and Grünbaum, 2006). Avoidance behavior has also been observed in

Journal of Experimental Biology (2021) 224, jeb239178. doi:10.1242/jeb.239178

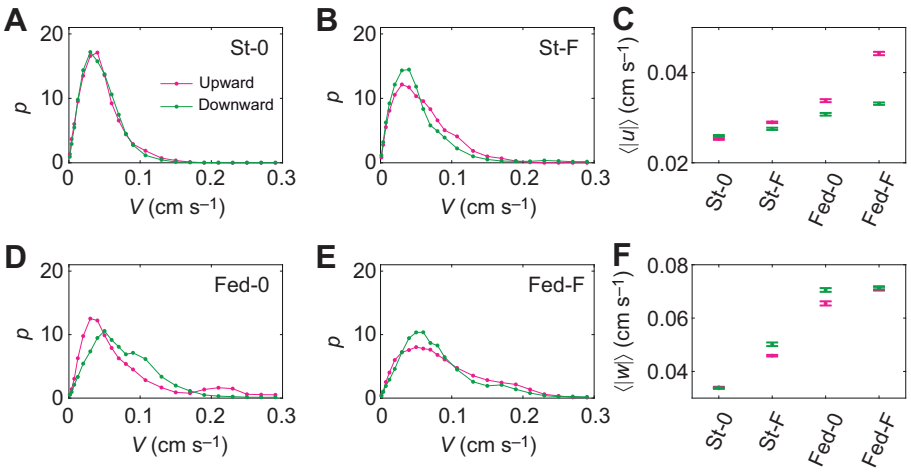

Fig. 6. Larval speed observations for upward- and downward-moving larvae. (A,B,D,E) Speed PDFs for all treatments for upward- and downward-moving larvae for all treatments. (C,F) Mean absolute horizontal $\langle|\boldsymbol{u}|\rangle$ (C) and vertical $\langle|\boldsymbol{w}|\rangle$ (F) velocity for upward- and downward-moving larvae for all treatments. Error bars indicate 95% confidence intervals. The treatments refer to starved larvae without or with food (St-0, St-F), and previously fed larvae without or with food (Fed-0, Fed-F).

copepods when presented with a thin layer of chemical toxins from harmful algae in the laboratory (True et al., 2018). In our observations, while horizontal velocity magnitude (Fig. 3A) and frequency of horizontal movement (Fig. 5B) increased in the presence of food for all larvae, increases in vertical swimming magnitude and frequency were also observed in the presence of food for the starved larvae. Therefore, we found that starved larvae met their increased horizontal motion with an increase in their vertical motion, and aggregation was not observed. However, we note that the experiments of Menden-Deuer and Grünbaum (2006) explicitly used phytoplankton in a thin layer, whereas we used a well-mixed concentration. It remains to be seen whether *C. fornicata* would exhibit aggregation behavior when encountering a thin layer of food, and we recommend future laboratory experiments to explore this hypothesis.

Overall speed of the larvae also increased in the presence of food for both the previously fed and starved larvae. In this case, speed includes both passive motion owing to sinking and active motion owing to swimming. However, the swimming effort can be partially isolated. We found the average upward vertical velocity of the larvae increased with the presence of food in all treatments (see Fig. 6F); this is direct evidence of increased swimming effort in response to food. We also saw increases of horizontal velocity magnitudes in the presence of food in both fed and starved treatments, another direct result of increased horizontal swimming effort (see Fig. 3A). The largest increase in horizontal velocity magnitude was seen for the larvae traveling upward (Fig. 6C). These observations show that larvae increased both their vertical and horizontal swimming efforts in the presence of food, thus indicating a direct link between foraging and increased swimming speed. Although there was no direct observation of feeding in this study, the measurements of larval velocity in the presence of food suggest that the larvae can feed without any reduction of swimming speed.

The amount of vertical larval motion also changed across treatments (see Fig. 5B). Compared with the treatments without food, the starved larvae in food were observed moving vertically more often, and the fed larvae in food were observed moving vertically an equal amount. This does not agree with the hypothesis that vertical swimming is an appropriate foraging strategy to encounter horizontal thin layers of food in the ocean environment. The starved larvae without food would theoretically be more desperate to encounter food and swim vertically, yet it was the fed larvae without food that exhibited the highest fraction of vertical motion. The fed larvae exhibited an effective foraging strategy in the absence of food by increasing their swimming anisotropy with a high frequency of vertical motion and a low frequency of horizontal motion. This discrepancy between the fed and starved larvae observations may be explained by an energy-conserving strategy of depth-keeping for the starved larvae in the absence of food.

Our observations further demonstrate differences in the shape of the distributions of horizontal and vertical velocity. Across all treatments, the horizontal velocity distributions of the larvae are

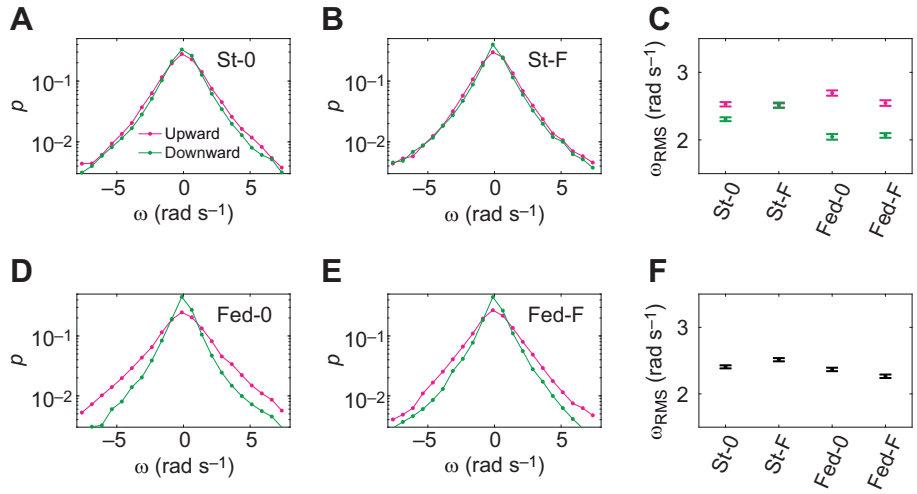

Fig. 7. Larval angular velocity observations for upward- and downward-moving larvae. (A,B,D,E) Larval angular velocity ω PDFs for all treatments for upward- and downward-moving larvae. (C,F) Corresponding ω_{RMS} for all treatments for upward- and downward-moving larvae (C), and total ω_{RMS} for all larvae (F). Error bars indicate 95% confidence intervals. Similar to Fig. 6, the treatments refer to starved larvae without or with food (St-0, St-F), and previously fed larvae without or with food (Fed-0, Fed-F).

more isotropic and normally distributed than the vertical velocities. This suggests that larvae may have more diffusive-type motion in the horizontal direction than in the vertical direction, which agrees with observations of marine protists in the laboratory (Schuech and Menden-Deuer, 2014). In addition, it illustrates fundamental differences in vertical and horizontal behavior, as expected. Vertical migration controls how larvae disperse in sheared ocean currents, and spending more time at the surface when feeding might mean larvae are exposed to faster currents that could affect their dispersal distance. Horizontal motion of larvae is more likely to influence how larvae interact with their local environment, for example when settling. Side-to-side motion when swimming in helices may help larvae locate settlement cues (Maciejewski et al., 2019) and can influence dispersal over small spatial scales in calm waters (Bingham and Young, 1991).

Changes in the vertical distribution of larvae were also observed in response to food, with the strongest response for the starved larvae. Overall, larvae were observed higher in the flasks in the presence of food in both treatments. This is consistent with previous work that found changes in vertical distribution as a response to food for other larval species (Metaxas and Young, 1998; Arellano et al., 2012). The vertical distribution calculations in the present study included larvae at the bottom of the flasks that were not swimming. Thus, not only did the presence of food alter how the observed larvae swam, it affected their swimming propensity. Larvae that remain near the seafloor tend to disperse less (Shanks, 2009). In contrast, foraging behavior can reduce larval dispersal distances by an order of magnitude relative to distances predicted by passive transport (Woodson and McManus, 2007).

Our observations correspond with the anatomical swimming structure of larval *C. fornicata*. Specifically, the distinction between behaviors in the vertical and horizontal dimensions are most likely due in part to anatomical constraints on veliger swimming. *Crepidula fornicata* larvae and other veligers have a heavy shell; this shell provides a torque that keeps the larvae oriented with the velum pointed upward (Chan et al., 2013). This torque biases the larvae to produce propulsion upward most often when swimming. Also, because larval *C. fornicata* are negatively buoyant, they must actively swim upward, but can passively sink downward. We hypothesized that the difference in active and passive behaviors would create an anisotropy in vertical behaviors. As expected, the upward- and downward-moving behaviors of larvae showed differences across most treatments. Specifically, angular velocity and horizontal speed of the upward-moving larvae were larger than or equal to those of the downward-moving larvae (Figs 6C and 7C), illustrating more active behavior when swimming upward.

The shell of *C. fornicata* grows as the larvae mature (Pechenik, 1984), so swimming anisotropy may also be a function of age. In a previous study, *C. fornicata* larvae swam fastest at 6 days post-hatching, with older larvae swimming more slowly and exhibiting more settlement behavior (Chan et al., 2013). Swimming speed in *C. fornicata* larvae depends most heavily on velum size (Chan et al., 2013). Velum size can be influenced by food availability during growth, as the velum of *C. fornicata* has been observed to grow faster under reduced food concentrations (Klinzing and Pechenik, 2000). In this work, we found similar responses to food regardless of feeding history. Specifically, a similar increase in larval speed magnitude for both starved and fed larvae (0.0078 and 0.0068 cm s^{-1}, respectively) was observed, suggesting that starvation history is not as important as the intrinsic behavioral response to food availability.

In many studies, observations of larval swimming behavior are presented as average values, either averaged across individuals or over time. Our results reveal that averaged values, which lack information about the range of observed behaviors, do not properly represent larval behavior. For example, the mean horizontal velocities for larvae in each treatment are zero, but the RMS values are non-zero and show a clear trend. In a vertically constricted experiment, average vertical velocities also are not as representative of behavior as vertical distributions. In addition, averaging inherently filters the data, removing information. Behavior of *C. fornicata* is unsteady, so describing it with average values does not capture the full range of observed behaviors. Because individual behaviors are often difficult to classify, we recommend using distributions of velocity as well as anisotropy indicators to continually assess responses to environmental cues.

As accuracy and resolution in hydrodynamic simulations improve, it is important to include realistic models of behavior (Metaxas and Saunders, 2009). Therefore, we must continually reassess how well existing models capture real larval behaviors and where they may fall short. Behavior is intrinsically linked to dispersal, so future modeling studies should include more refined models of larval behavior in the field, including increased swimming speed, increased horizontal swimming and higher vertical position in the water column of *C. fornicata* when food sources are encountered.

Acknowledgements
We thank Jan Pechenik (Tufts University) for assistance in culturing *Crepidula fornicata* larvae and Anthony Pires (Dickinson College) for helpful discussions over the course of this work. We also thank the anonymous reviewers for their valuable comments, which have greatly improved the paper.

Competing interests
The authors declare no competing or financial interests.

Author contributions
Conceptualization: M.H.D., K.S.M.-K., B.T., J.D.W., L.M.; Methodology: M.H.D., K.S.M-K., B.T., J.D.W., L.M.; Software: M.H.D., J.D.W.; Validation: M.H.D., K.S.M.-K.; Formal analysis: M.H.D., K.S.M.-K., J.D.W.; Investigation: B.T.; Resources: L.M.; Data curation: M.H.D.; Writing - original draft: M.H.D., K.S.M.-K.; Writing - review & editing: M.H.D., K.S.M.-K., B.T., J.D.W., L.M.; Visualization: M.H.D.; Supervision: L.M.; Project administration: L.M.; Funding acquisition: L.M.

Funding
M.H.D. and K.S.M.-K. were supported by postdoctoral scholarships from Woods Hole Oceanographic Institution, and B.T. was supported by a WHOI Summer Student Fellowship. This work was also supported by National Science Foundation grant OCE-0850419.

Data availability
Trajectory data for the larvae can be found online at https://figshare.com/s/8219412b0e6a4cd8e7c6, and are also available from BCO-DMO at https://doi.org/10.26008/1912/BCO-DMO.834221.1.

Supplementary information
Supplementary information available online at https://jeb.biologists.org/lookup/doi/10.1242/jeb.239178.supplemental

References
Arellano, S. M., Reitzel, A. M. and Button, C. A. (2012). Variation in vertical distribution of sand dollar larvae relative to haloclines, food, and fish cues. *J. Exp. Mar. Biol. Ecol.* **414**, 28-37. doi:10.1016/j.jembe.2012.01.008

Bingham, B. L. and Young, C. M. (1991). Larval behavior of the ascidian *Ecteinascidia turbinata* Herdman; an in situ experimental study of the effects of swimming on dispersal. *J. Exp. Mar. Biol. Ecol.* **145**, 189-204. doi:10.1016/0022-0981(91)90175-V

Butman, C. A., Grassle, J. P. and Webb, C. M. (1988). Substrate choices made by marine larvae settling in still water and in a flume flow. *Nature* **333**, 771-773. doi:10.1038/333771a0

Chan, K. Y. K. (2012). Biomechanics of larval morphology affect swimming: Insights from the sand dollars *Dendraster excentricus*. *Integr. Comp. Biol.* **52**, 458-469. doi:10.1093/icb/ics092

Chan, K. Y. K., Jiang, H. and Padilla, D. K. (2013). Swimming speed of larval snail does not correlate with size and ciliary beat frequency. *PLoS ONE* **8**, 6-13. doi:10.1371/journal.pone.0082764
Cowen, R. K. and Sponaugle, S. (2009). Larval dispersal and marine population connectivity. *Ann. Rev. Mar. Sci.* **1**, 443-466. doi:10.1146/annurev.marine.010908.163757
Daigle, R. M. and Metaxas, A. (2012). Modeling of the larval response of green sea urchins to thermal stratification using a random walk approach. *J. Exp. Mar. Biol. Ecol.* **438**, 14-23. doi:10.1016/j.jembe.2012.09.004
Daro, M. (1988). Migratory and grazing behavior of copepods and vertical distribution of phytoplankton. *Bull. Mar. Sci.* **43**, 710-729.
Durham, W. M. and Stocker, R. (2012). Thin phytoplankton layers: characteristics, mechanisms, and consequences. *Ann. Rev. Mar. Sci.* **4**, 177-207. doi:10.1146/annurev-marine-120710-100957
Efron, B. (1979). Bootstrap methods: another look at the jackknife. *Ann. Stat.* **7**, 1-26.
Emlet, R., Strathman, R. and Strickler, J. (1985). Gravity, drag, and feeding currents of small zooplankton. *Science* **228**, 1016-1017. doi:10.1126/science.228.4702.1016
Fuchs, H. L., Mullineaux, L. S. and Solow, A. R. (2004). Sinking behavior of gastropod larvae (*Ilyanassa obsoleta*) in turbulence. *Limnol. Oceanogr.* **49**, 1937-1948. doi:10.4319/lo.2004.49.6.1937
Fuchs, H. L., Hunter, E. J., Schmitt, E. L. and Guazzo, R. A. (2013). Active downward propulsion by oyster larvae in turbulence. *J. Exp. Biol.* **216**, 1458-1469. doi:10.1242/jeb.079855
Fuchs, H. L., Christman, A. J., Gerbi, G. P., Hunter, E. J. and Diez, F. J. (2015). Directional flow sensing by passively stable larvae. *J. Exp. Biol.* **218**, 2782-2792. doi:10.1242/jeb.125096
Fuchs, H. L., Gerbi, G. P., Hunter, E. J. and Christman, A. J. (2018). Waves cue distinct behaviors and differentiate transport of congeneric snail larvae from sheltered versus wavy habitats. *Proc. Natl. Acad. Sci. USA* **115**, E7532-E7540. doi:10.1073/pnas.1804558115
Gallager, S. M. (1988). Visual observations of particle manipulation during feeding in larvae of a bivalve mollusc. *Bull. Mar. Sci.* **43**, 344-365.
Gilpin, W., Prakash, V. N. and Prakash, M. (2017). Vortex arrays and ciliary tangles underlie the feeding–swimming trade-off in starfish larvae. *Nat. Phys.* **13**, 380-386. doi:10.1038/nphys3981
Henry, J. J., Collin, R. and Perry, K. J. (2010). The slipper snail, *Crepidula*: an emerging lophotrochozoan model system. *Biol. Bull.* **218**, 211-229. doi:10.1086/BBLv218n3p211
Kelley, D. H. and Ouellette, N. T. (2011). Using particle tracking to measure flow instabilities in an undergraduate laboratory experiment. *Am. J. Phys.* **79**, 267-273. doi:10.1119/1.3536647
Kessler, J. O. (1986). Individual and collective fluid dynamics of swimming cells. *J. Fluid Mech.* **173**, 191-205. doi:10.1017/S0022112086001131
Klinzing, M. S. E. and Pechenik, J. A. (2000). Evaluating whether velar lobe size indicates food limitation among larvae of the marine gastropod *Crepidula fornicata*. *J. Exp. Mar. Biol. Ecol.* **252**, 255-279. doi:10.1016/S0022-0981(00)00245-8
Koehl, M. (2007). Mini review: hydrodynamics of larval settlement into fouling communities. *Biofouling* **23**, 357-368. doi:10.1080/08927010701492250
Maciejewski, M. F., Meyer, K. S., Wheeler, J. D., Anderson, E. J., Pittoors, N. C. and Mullineaux, L. S. (2019). Helical swimming as an exploratory behavior in competent larvae of the eastern oyster (*Crassostrea virginica*). *J. Exp. Mar. Biol. Ecol.* **510**, 86-94. doi:10.1016/j.jembe.2018.10.007
Mahjoub, M. S., Souissi, S., Schmitt, F. G., Nan, F. H. and Hwang, J. S. (2011). Anisotropy and shift of search behavior in Malabar grouper (*Epinephelus malabaricus*) larvae in response to prey availability. *Hydrobiologia* **666**, 215-222. doi:10.1007/s10750-010-0549-4
McManus, M. A. and Woodson, C. B. (2012). Plankton distribution and ocean dispersal. *J. Exp. Biol.* **215**, 1008-1016. doi:10.1242/jeb.059014
Menden-Deuer, S. and Grünbaum, D. (2006). Individual foraging behaviors and population distributions of a planktonic predator aggregating to phytoplankton thin layers. *Limnol. Oceanogr.* **51**, 109-116. doi:10.4319/lo.2006.51.1.0109
Metaxas, A. (2001). Behaviour in flow: perspectives on the distribution and dispersion of meroplanktonic larvae in the water column. *Can. J. Fish. Aquat. Sci.* **58**, 86-98. doi:10.1139/f00-159
Metaxas, A. and Saunders, M. (2009). Quantifying the "bio-" components in biophysical models of larval transport in marine benthic invertebrates: advances and pitfalls. *Biol. Bull.* **216**, 257-272. doi:10.1086/BBLv216n3p257
Metaxas, A. and Young, C. M. (1998). Responses of echinoid larvae to food patches of different algal densities. *Mar. Biol.* **130**, 433-445. doi:10.1007/s002270050264
Meyer, K. S., Wheeler, J. D., Houlihan, E. and Mullineaux, L. S. (2018). Desperate planktotrophs: decreased settlement selectivity with age in competent eastern oyster *Crassostrea virginica* larvae. *Mar. Ecol. Prog. Ser.* **599**, 93-106. doi:10.3354/meps12653
Okubo, A. (1994). The role of diffusion and related physical processes in dispersal and recruitment of marine populations. *The Bio-Physics of Marine Larval Dispersal* **45**, 5-32. doi:10.1029/CE045p0005
Pechenik, J. A. (1984). The relationship between temperature, growth rate, and duration of planktonic life for larvae of the gastropod *Crepidula fornicata* (L.). *J. Exp. Mar. Biol. Ecol.* **74**:241-257. doi:10.1016/0022-0981(84)90128-X
Pernet, B. (2018). *Larval Feeding: Mechanisms, Rates, and Performance in Nature*. Oxford: Oxford University Press.
Pineda, J. and Reyns, N. (2018). Larval transport in the coastal zone: biological and physical processes. In *Evolutionary Ecology of Marine Invertebrate Larvae* (ed. T. J. Carrier, A. M. Reitzel and A. Heyland), pp. 145-163. New York: Oxford University Press. doi:10.1093/oso/9780198786962.003.0011
Porch, C. E. (1998). A theoretical comparison of the contributions of random swimming and turbulence to absolute dispersal in the sea. *Bull. Mar. Sci.* **62**, 31-44.
Sameoto, J. A. and Metaxas, A. (2008). Interactive effects of haloclines and food patches on the vertical distribution of three species of temperate invertebrate larvae. *J. Exp. Mar. Biol. Ecol.* **367**, 131-141. doi:10.1016/j.jembe.2008.09.003
Schuech, R. and Menden-Deuer, S. (2014). Going ballistic in the plankton: anisotropic swimming behavior of marine protists. *Limnol. Oceanogr.* **4**, 1-16. doi:10.1215/21573689-2647998
Shanks, A. L. (1995). Orientated swimming by megalopae of several eastern north pacific crab species and its potential role in their onshore migration. *J. Exp. Mar. Biol. Ecol.* **186**, 1-16. doi:10.1016/0022-0981(94)00144-3
Shanks, A. L. (2009). Pelagic larval duration and dispersal distance revisited. *Biol. Bull.* **216**, 373-385. doi:10.1086/BBLv216n3p373
Strathmann, R. R. and Grünbaum, D. (2006). Good eaters, poor swimmers: compromises in larval form. *Integr. Comp. Biol.* **46**, 312-322. doi:10.1093/icb/icj031
Strathmann, R. R., Brante, A. and Oyarzun, F. X. (2019). Contrasting metatrochal behavior of mollusc and annelid larvae and the regulation of feeding while swimming. *Biol. Bull.* **236**, 130-143. doi:10.1086/701730
True, A. C., Webster, D. R., Weissburg, M. J. and Yen, J. (2018). Copepod avoidance of thin chemical layers of harmful algal compounds. *Limnol. Oceanogr.* **63**, 1041-1055. doi:10.1002/lno.10752
Visser, A. W. and Kiørboe, T. (2006). Plankton motility patterns and encounter rates. *Oecologia* **148**, 538-546. doi:10.1007/s00442-006-0385-4
von Dassow, G., Emlet, R. and Grünbaum, D. (2017). Boundary effects on currents around ciliated larvae. *Nat. Phys.* **13**, 520-521. doi:10.1038/nphys4154
Wheeler, J. D., Helfrich, K. R., Anderson, E. J. and Mullineaux, L. S. (2015). Isolating the hydrodynamic triggers of the dive response in eastern oyster larvae. *Limnol. Oceanogr.* **60**, 1332-1343. doi:10.1002/lno.10098
Wheeler, J. D., Luo, E., Helfrich, K. R., Anderson, E. J., Starczak, V. R. and Mullineaux, L. S. (2017). Light stimulates swimming behavior of larval eastern oysters *Crassostrea virginica* in turbulent flow. *Mar. Ecol. Prog. Ser.* **571**, 109-120. doi:10.3354/meps12106
Woodson, C. and McManus, M. (2007). Foraging behavior can influence dispersal of marine organisms. *Limnol. Oceanogr.* **52**, 2701-2709. doi:10.4319/lo.2007.52.6.2701
Yen, J. (1988). Directionality and swimming speeds in predator-prey and male-female interactions of *Euchaeta rimana*, a subtropical marine copepod. *Bull. Mar. Sci.* **43**, 395-403.
Young, C. and Chia, F.-S. (1984). Microhabitat-associated variability in survival and growth of subtidal solitary ascidians during the first 21 days after settlement. *Mar. Biol.* **81**, 61-68. doi:10.1007/BF00397626
Young, C. M. and Vazquez, E. (1995). Morphology, larval development, and distribution of *Bathypera feminalba* n. sp. (Ascidiacea: Pyuridae), a deep-water ascidian from the fjords and sounds of British Columbia. *Invertebr. Biol.* **114**, 89-106. doi:10.2307/3226958

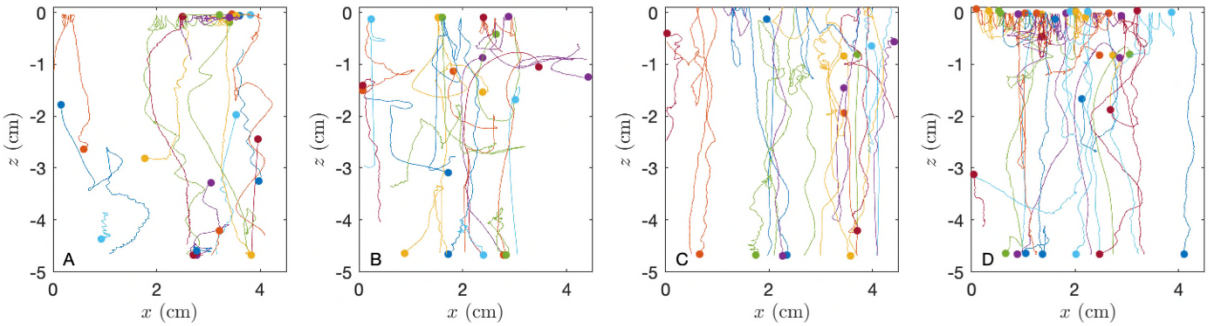

Fig. S1. *All measured trajectories of larvae from one replicate for each treatment (St-0, St-F, Fed-0, Fed-F) in the plots from left to right respectively. The dots represent the starts of each individual track. Individual larvae may correspond to multiple tracks if they have a pause in their tracking due to interactions with the top or bottom of the flask.*

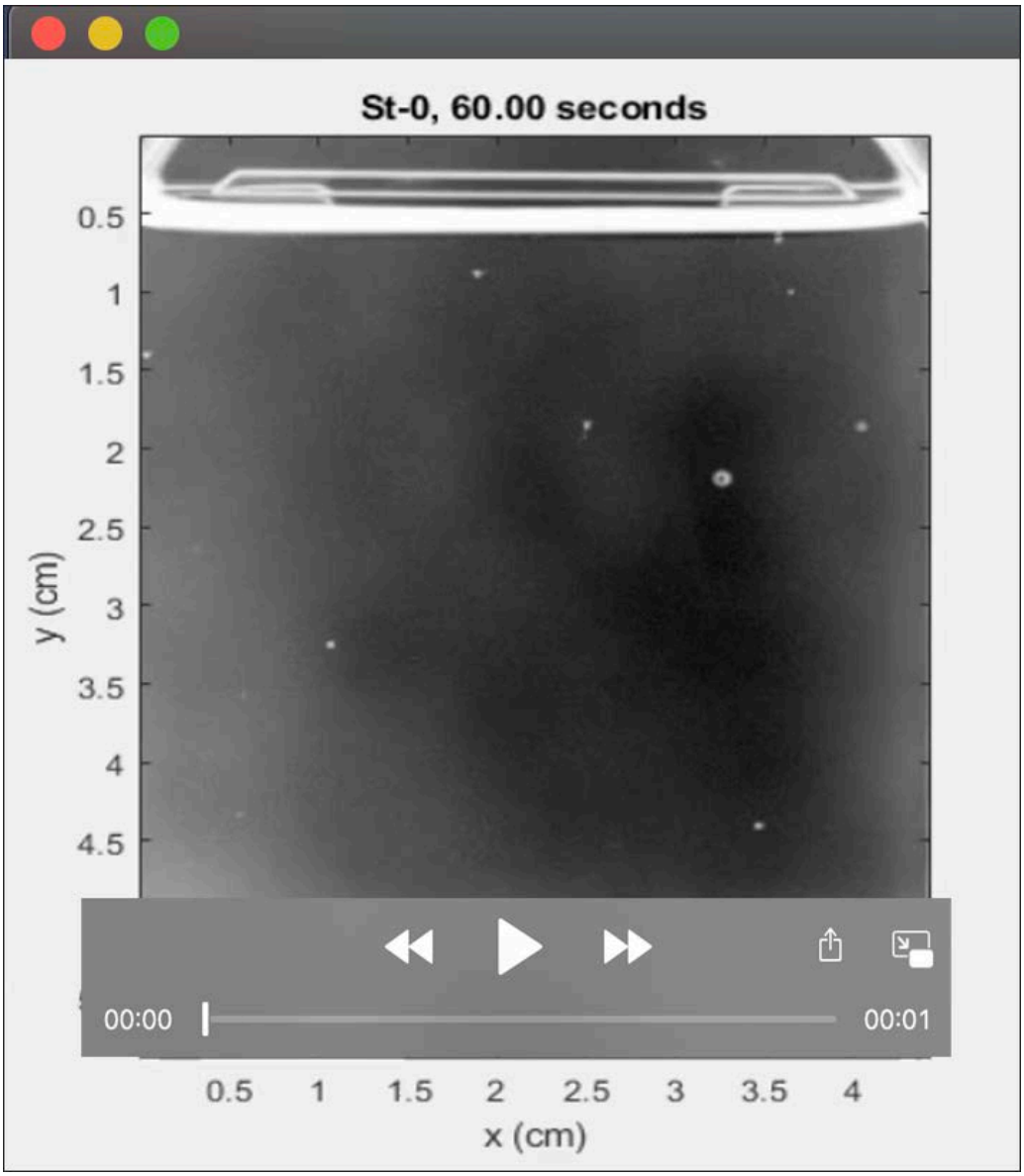

Movie 1. *Corresponding video footage from St experimental trials shown in Fig. S1. Images are compressed, and every 5th frame is plotted in time. Playback is increased 2X in speed. Two minutes of footage from the total five minute experiment are shown for each trial. The first minute of the movie shows footage from one St-0 trial, and the second minute shows footage from one St-F trial. Trajectories of the larvae from the tracking data are plotted on top of the image data.*

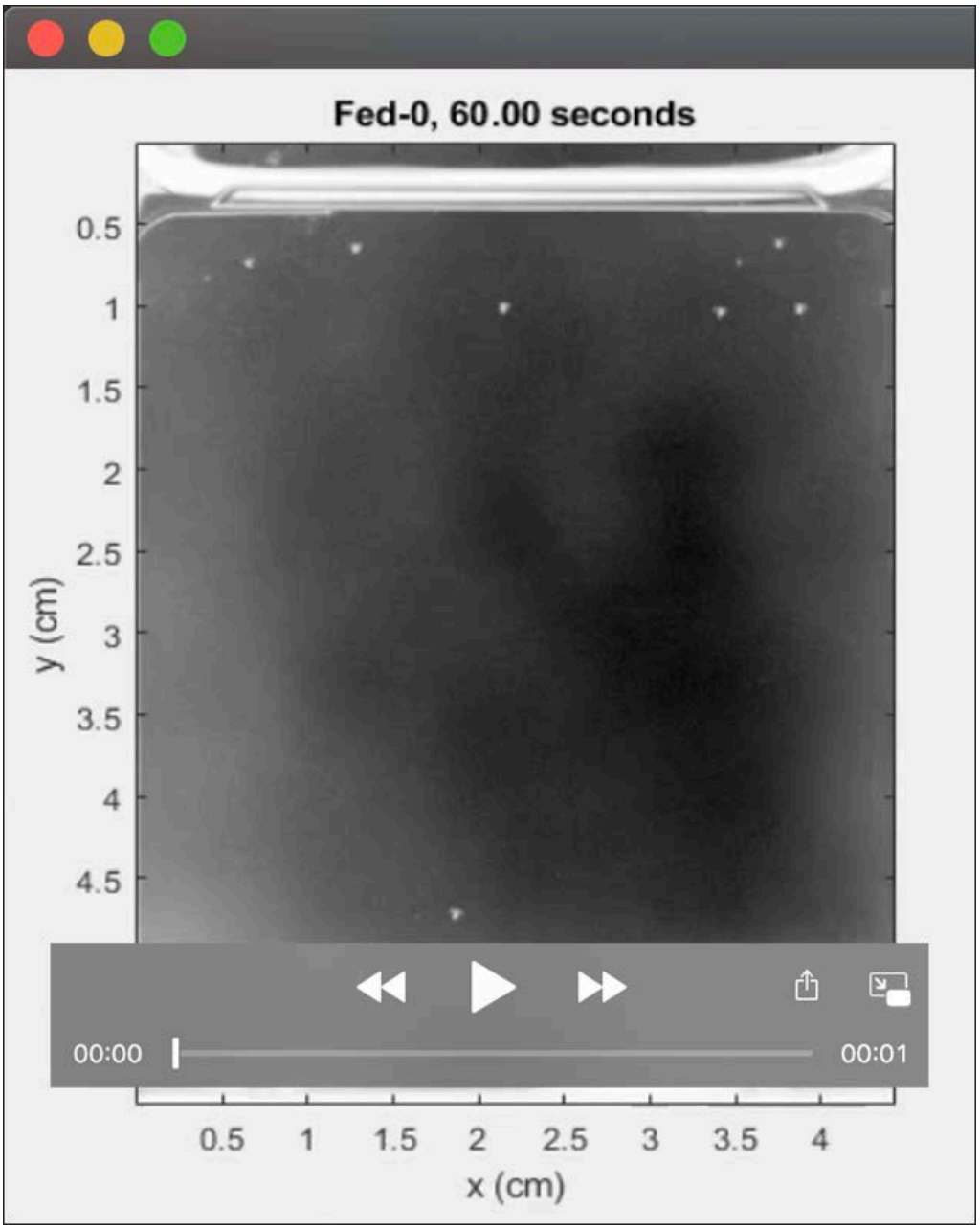

Movie 2. *Corresponding video footage from Fed experimental trials shown in Fig. S1. Images are compressed, and every 5th frame is plotted in time. Playback is increased 2X in speed. Two minutes of footage from the total five minute experiment are shown for each trial. The first minute of the movie shows footage from one Fed-0 trial, and the second minute shows footage from one Fed-F trial. Trajectories of the larvae from the tracking data are plotted on top of the image data.*